ALMA Memo No. 317
Comparison of the antenna pointing error effect on the image quality for two configurations and two source types.

L. Kogan[1]

(1) - National Radio Astronomy Observatory, Socorro, New Mexico, USA

August 2, 2000

Abstract

Observation of the two source models: M51 with spiral expanded structure and methanol masers with cluster of compact sources, has been simulated, observed by the two arrays of 64 antennas (12 meter diameter each) at snapshot mode with random pointing error of the antennas. The two configurations: the doughnut and the ring have been considered. The size of the source is equal to a half of the antenna primary beam. The rms of the pointing error was in the range (0-20)% of the primary beam width. The quality of the restored image is aggravated with increasing the pointing error. The better of the two configuration stays to be better for any pointing error although the difference is becoming small for the large pointing error.

1 Simulation

In their fundamental paper ([1]) Cornwell, Holdaway, and Uson showed that pointing error of array antennas can aggravate the quality of the image very seriously. Morita-san ([2]) carried out the simulation of the pointing error comparing a spiral configuration and ring with sum of Gaussian components as the model. He showed that even small pointing error aggravates the quality of the image very much for the both configurations. In this memo I want to answer on the question: Can estimation of a configuration based on the simulation without pointing error lead to the wrong choice because the pointing error can inverse our idea about the superiority of the configuration?

In the simulation I have compared the doughnut type configuration, optimized minimizing side lobes inside of the circle of radius 20 synthesized beams; and the ring configuration. The radius of the ring configuration was adjusted to get the same resolution as the resolution of the doughnut configuration.

The first selected model was taken from the observation of the methanol maser at DR21(OH) conducted at VLA at $\lambda = 7$mm ([3]). The image is represented by the cluster of compact sources with the most power component located at the center of the map and other components located unsymmetry at the left part of the map. The total size of the map is 25"x25". The wavelength of the simulation was selected as 3mm to get the primary beam of the 12 meter dish twice bigger the image size. The primary beam pattern corresponds to the illumination of the circular dish with 10 db down at its edge. Such an illumination is planned for the future ALMA's antenna (P. Napier, private communication).

The second selected model (expanded) is the spiral galaxy M51. The image was given to me by John Conway. The size of this image is 5"x5". The wavelength was selected 5 times less to get the same ratio (2) of the primary beam width to the model size.

The AIPS task UVCON has been used for simulation of the UV data and several other standard AIPS tasks have been used in the process: IMAGR to create the image based on the simulated UV data; COMB to create the difference between the model image used in UVCON and the image restored by IMAGR; IMEAN to estimate the rms of the difference map; and other auxiliary tasks. Using UVCON in simulation the pointing error is limited by the model presented as a sum of the clean components. So I used UVCON with model presented by the image simulating the UV data. Then I used IMAGR to create the secondary model presented my the clean components. The AIPS task IMAGR creates the image that is the sum of the clean components convolved with the beam and the residual. For the following comparison of the restored image and the model I had to create the model represented by the clean components convolved with the beam excluding the residual, because the UVCON uses the clean components as a model (without the residual). To create such a model I superimposed the map represented by clean components (task RSTOR) on the zero map. The zero map was created by subtracting two identical images (task COMB). The negative clean components were eliminated using the task CCEDT. The final models used in simulation are shown at the figures (1, 2). The size of the convolution beam was selected identical at the stage of creating the model (RSTOR) and at the stage of restoring the image (IMAGR). It was 200 milliarcsec for the model of the compact source cluster and 100 milliarcsec for the expanded source model M51.

To judge image quality, I used the criterion **FIDR** defined as the image peak divided by the rms of the difference (model image-restored image) map, using the whole map. This criterion is the modified dynamic range **DR** defined at ([1]) as the image peak divided by the rms of the difference (model image-restored image) map, using the off-source area. The **FIDR** estimates both the fidelity and the dynamic range of the restored image. I had a problem using the fidelity index **FI** defined at ([1]) as the mean of the ratio of the model to the difference, because the division creates big pikes when the dominator is close to zero.

2 Discussion

The result of the simulation is given at the table 1 for the cluster model and at the table 2 for the expanded (M51) model. The pointing error is implemented as a random for different antennas and in time. The pointing error given in the tables is in the rms of the random error. As expected ([4]) doughnut configuration gives better image quality for the both model.

The first model is rather simple and the snaphot observation with the both configurations gives a small deconvolution errors. So the image quality (**FIDR**) is high for the first model in absence of the pointing error for the both configurations with the visible superiority of the doughnut. The image quality (**FIDR**) drops down several times with pointing error of 1% of the primary beam and stays on the same level with a small superiority of the doughnut. Such a result is obtained by ([2]) also. It looks like the deconvolution error and pointing error are added in square. So when deconvolution error is small because of a good UV coverage and absence of the thermal noise, the pointing error dominates even when it is small.

The second model is too complicate for the snapshot observation and so the image quality (**FIDR**) is not so high in absence of the pointing error. The deconvolution error is not small at this case, the pointing error does not dominate and therefore the image quality does not drop so much (as it is for the first model) with pointing error including. The image quality (**FIDR**) with doughnut decreases from 580 till 107 when error pointing increases from zero to 20% of the primary beam. For the ring the image quality (**FIDR**) does not change with the pointing error increasing staying at the level of 70, because the deconvolution error dominates at this case. The image quality (**FIDR**) with the doughnut is several times better than with the ring at the pointing error range (0-10)%.

Comparing the effect of the pointing error on the image quality for the two configuration we are coming to the conclusions:
The configuration that gives better image without pointing error remains be better with the same pointing error.
The pointing error aggravates the image quality more seriously for the better quality image without pointing error.

Table 1: The image quality (**FIDR**) as a function of pointing error for the cluster model. Primary beam (PRBEAM) is equal 50 arcsec.

Error, arcsec	0	0.5	1	2.5	5	10
Error, % to PRBEAM	0	1	2	5	10	20
Doughnut	34860	6030	6016	5107	2718	1131
Ring	16510	5941	5691	5220	2581	1105

Table 2: The image quality (**FIDR**) as a function of pointing error for the expanded (M51) model. Primary beam (PRBEAM) is equal 10 arcsec.

Error, arcsec	0	0.1	0.2	0.5	1	2
Error, % to PRBEAM	0	1	2	5	10	20
Doughnut	580	408	400	345	267	107
Ring	71	69	70	69	68	60

3 Conclusion

The observation of two different classes of sources (cluster of compact sources and expanded source) with two configurations (doughnut and ring) has been simulated with pointing error of the antennas.
Comparing the effect of the pointing error on the image quality for the two configurations we are coming to the conclusion:
The configuration that gives better image without pointing error remains be better with the same pointing error.
The pointing error aggravates the image quality more seriously for the better quality image without pointing error.
For some sources the difference of the image quality for different configurations can become very small in presence of the pointing error. So the Holdaway's precaution is partially right although there is no inversion. His statement can be paraphrased :
The pointing error can destroy a difference between configurations in the sense of the image quality. Take any configuration and get equally bad image quality.

References

[1] T.J. Cornwell, M.A. Hodaway, and J.M. Uson, Radio-interferometric imaging of very large objects, A&A, v 271, p 697, 1993

[2] Koh-Ichiro Morita, Imaging simulations including pointing error for single pointing imaging. http://www.tuc.nrao.edu/ kmorita/CONFIG/PERR2.html

[3] L. Kogan,and V. Slysh, VLA imaging of class I methanol masers at 7 millimeters with angular resolution $\sim 0''.2$. the Astrophysical Journal 497,800-806, 1998

[4] L.R. Kogan, MMA memo 247, The Imaging Characteristics of an Array with Minimum Side Lobes. I. 1999

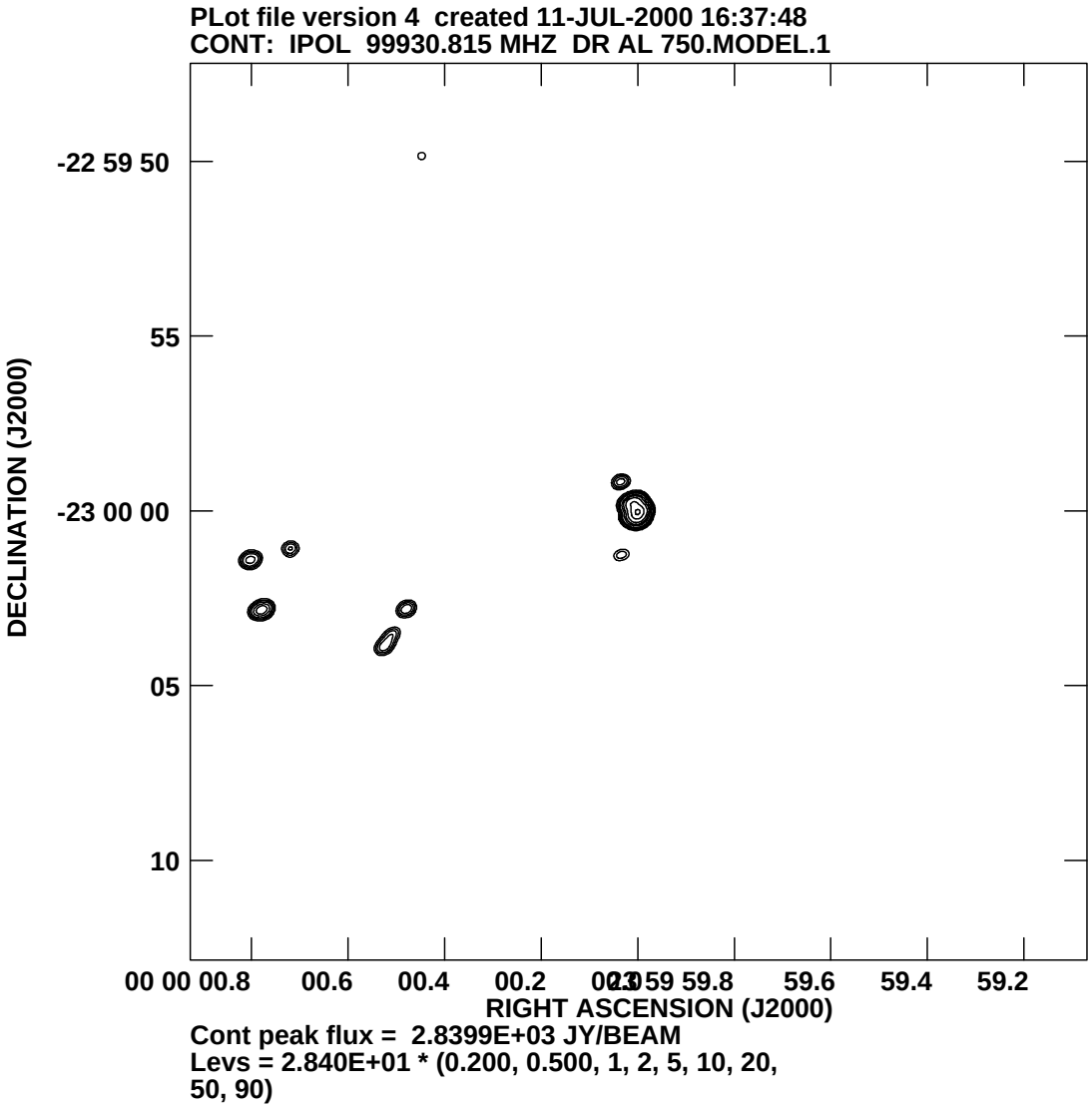

Figure 1: Model as a cluster of compact sources used at the simulation. Wavelength is 3mm. The convolution beam is 200x200 milliarcsec.

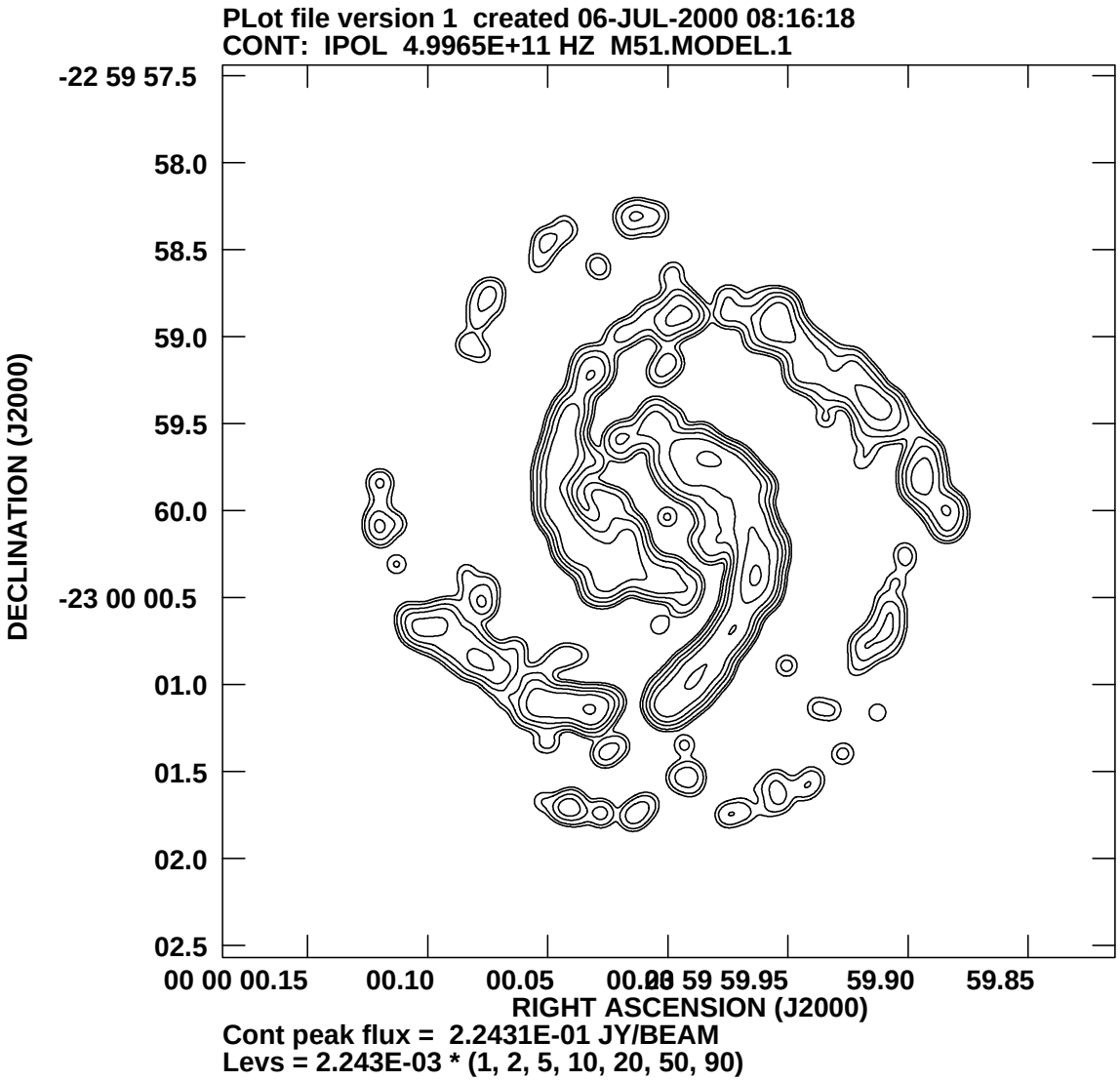

Figure 2: Model as the spiral galaxy M51 used at the simulation. Wavelength is 0.06mm. The convolution beam is 100x100 milliarcsec.